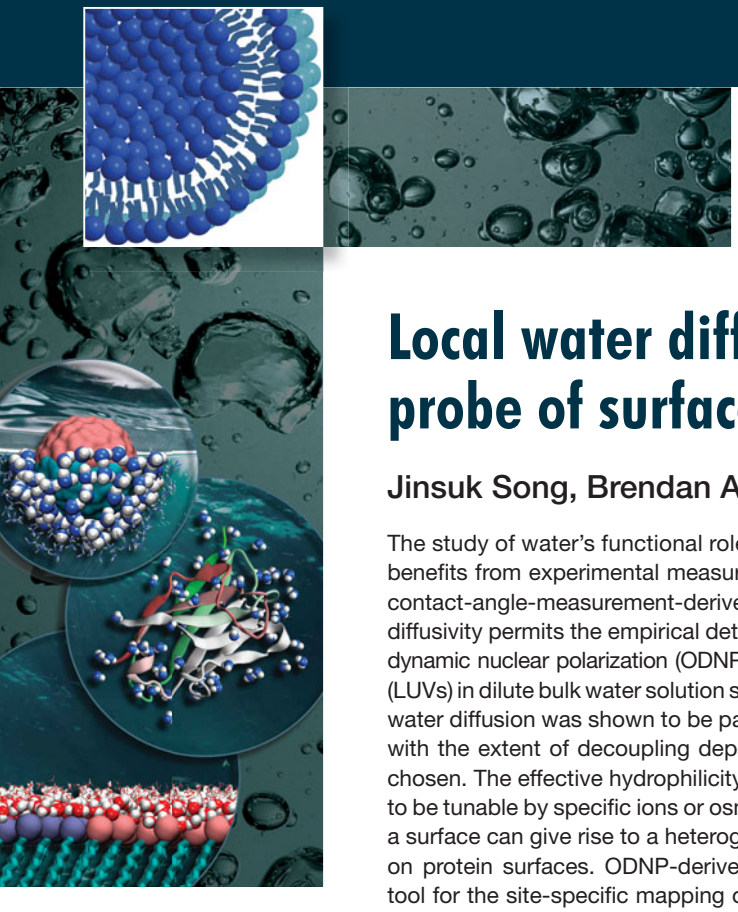


Local water diffusivity as a molecular probe of surface hydrophilicity

Jinsuk Song, Brendan Allison, and Songi Han

The study of water's functional role on hydrophilic surfaces of biological and soft materials benefits from experimental measurements that operate at finer length and time scales than contact-angle-measurement-derived surface wettability. We show that local translational diffusivity permits the empirical determination of local hydrophilicity by means of Overhauser dynamic nuclear polarization (ODNP) amplified ^{1}H NMR relaxometry. Large unilamellar vesicles (LUVs) in dilute bulk water solution serve as good model hydrophilic surfaces, and their surface water diffusion was shown to be partially or entirely decoupled from the bulk water viscosity, with the extent of decoupling dependent on the surface activity of the particular viscogen chosen. The effective hydrophilicity of a hydrated LUV surface in solution was further shown to be tunable by specific ions or osmolytes dissolved in solution, and the chemical makeup of a surface can give rise to a heterogeneous hydration dynamics landscape, as demonstrated on protein surfaces. ODNP-derived surface water diffusivity is suggested to be a unique tool for the site-specific mapping of the interaction landscape of a wide range of functional materials operating in aqueous solution, from wet adhesives to fuel cell membranes.

Introduction

Understanding the interaction of water with biological and soft material surfaces is critical to rationalizing and predicting basic functions and properties of hydrated surfaces.[1,2] Binding and adsorption events, the solubility of macromolecules, enzyme catalysis, the overall wettability of macroscopic surfaces, and ion or molecular transport through membrane materials can be modulated or influenced by the degree of attraction of water to—that is, the hydrophilicity of—the macromolecular or material surface. As demonstrated by the intuitive example of a protein whose function disappears upon dehydration and reappears upon rehydration,[3] hydrophilicity is a functional property mediated through a proximate water network,[4,5] the characteristics of which vary with the influence of this surface chemical property.[6,7]

If net surface wettability[8] is characterized by a common contact angle measurement and extrapolated to net surface hydrophilicity, the lower spatial boundary of this *ex situ* technique will be the minimum span and volume of a water droplet. However, the interaction between water and a realistic surface varies not just from surface to surface but also from site to site, at length scales encompassing a few water layers from the surface and chemical residues spanning less than 1 nm laterally.[9,10]

Such variability is not limited to the biological domain: Analogous hydrophilic or hydrophobic regions making up a heterogeneous protein surface landscape[11–13] or a soft material surface, such as those of cell membranes[11,14,15] and sulfonyl-group-decorated polymer electrolyte fuel cell membranes,[16] also display heterogeneous surface hydration dynamics with dramatically varying hydrophilicity characteristics across different chemical moieties, domains, water channels, and polymer backbones. Crucially, this variability can encode function-related properties of materials operating in aqueous environments, for example, mediating adsorption, chemical catalysis, or transport.[12–15] Thus, to elucidate a potentially functional role of surface water at material and macromolecular interfaces, an experimental approach to probe local surface hydrophilicity at the (sub-) nanometer scale, with high sensitivity, is crucial. However, note that an effective surface hydrophilicity probe, even if site-specifically resolved, incorporates multiple forces into a single measure—the adhesion of water molecules to the surface and the cohesion of water molecules near the surface in particular—as these forces determine, in concert, behaviors such as whether a foreign molecule is likely to approach a binding site protected by a repulsive hydration shell.

Jinsuk Song, Department of Chemistry and Biochemistry, University of California, Santa Barbara, USA; jsong@chem.ucsb.edu
Brendan Allison, Department of Chemistry and Biochemistry, University of California, Santa Barbara, USA; ballison@chem.ucsb.edu
Songi Han, Department of Chemistry and Biochemistry, University of California, Santa Barbara, USA; songi@chem.ucsb.edu
DOI: 10.1557/mrs.2014.254

© 2014 Materials Research Society
https://doi.org/10.1557/mrs.2014.254 Published online by Cambridge University Press

Local and interfacial water molecules involved in the solvation of such hydrophilic surfaces are generally highly dynamic and subject to constant breaking and re-forming of hydrogen bonds within the hydrogen-bonded water network,[17] with the strength of this network determining the translational diffusion coefficient of water.[14] Thus, except in cases in which water molecules are strongly bound or in glassy states, an increase in net attraction of water to a surface, concurrent with a stronger hydrogen-bond network between water molecules near the surface, will increase the diffusion activation energy barrier of water[7,18] and decrease the local water diffusion constant according to the Arrhenius relation.[19]

Generally, a more ordered and cohesive local water network that seamlessly integrates with the hydrophilic surface, with molecular-level perfection at the surface–water "seam," will increase the activation energy barrier for the diffusion of water that experiences the influence of the surface. A retardation factor (ρ_t) for the translational diffusivity of these water molecules near a surface of interest (up to approximately two to four water layers), as compared to the diffusivity of bulk water under solution conditions equal to those of the immersed surface, is a direct experimental measure of effective net surface hydrophilicity. This can be understood both as analogous to and as a departure from contact angle measurement, which reports on the competition, at a solid–water–air interface, between water's attraction to the surface and its cohesive attraction to itself, translated to microscopic scales as the slowing of diffusion due to the influence of adhesion and cohesion at the surface–water interface of an entirely water-immersed surface.

The emerging Overhauser dynamic nuclear polarization (ODNP) relaxometry technique, coupled with site-specific spin labeling (typically employing stable nitroxide radical probes to specific sites in proteins, lipid membranes, or soft materials for localizing the surface of interest), permits the measurement of the translational water diffusivity of water within 5–10 Å (two to four water layers) of a localized spin label that is either tethered to the surface or selectively imbibed in the local environment of the material systems of interest.[20–22] We first establish the basic principles of ODNP in the following section, discuss the implication of the measurements in terms of the hydration structures and dynamics around hydrophilic surfaces with topological and chemical heterogeneities, leading to heterogeneous hydrophilicity, and then make a connection between surface water dynamics and surface properties. We conclude with an outlook for ODNP-enabled exploration of surface hydrophilicity and function-related material properties.

Overhauser dynamic nuclear polarization relaxometry

The DNP phenomenon called the Overhauser effect, postulated in 1953 by Albert Overhauser,[23] is a mechanism by which the larger polarization of an electron spin ensemble can be transferred to adjacent nuclei, thus enhancing and inverting the NMR signal in solution. Consistent with its description as a hybrid technique of electron paramagnetic resonance (EPR) and nuclear magnetic resonance (NMR), ODNP involves the manipulation of EPR by microwave irradiation to initiate polarization transfer from the electron to nuclear spins in the presence of an external magnetic field, resulting in an altered NMR signal. When electron spin transitions are induced by microwave irradiation, nuclear spins that experience dipolar coupling to the flipping electron spins concurrently undergo an induced spin transition, invoking flip-flop transitions between the electron spin of a probe and ^{1}H nuclear spins of water.[23–25] If the irradiation of the electron spin transition yields quantitative saturation of the EPR spectrum, the induced nuclear spin flips mediated by the magnetic dipolar coupling between the electron and nuclear spins can lead to a large enhancement and inversion of the NMR signal, by up to 50% of the ratio of the electron spin to the nuclear spin gyromagnetic ratio, that is, by 658/twofold when ^{1}H nuclei are involved.[26,27] The rate of the dipolar coupling-induced flip-flop transition decays with the distance r between the magnetic dipoles as $\sim r^{-6}$, so that the contributions of ^{1}H spins of water within ~10 Å of the electron spin are dominant.[28] Effective spin transitions occur when the changes in distance between electron and proton nuclear spins occur rapidly relative to the EPR frequency,[24,29] which implies that faster molecular dynamics of ^{1}H-bearing molecules, such as water, will enhance the ODNP efficiency.

In our implementation of ODNP, we focus on the coupling between the unpaired electron of a stable nitroxide radical probe tethered to or imbibed near macromolecular and material surfaces and the water molecules hydrating these surfaces. Thus, the experimental implementation of ODNP requires the incorporation of Heisenberg spin exchange and nitrogen nuclear spin relaxation, pertinent to the nitroxide radical probes, into the modeling and determination of their EPR saturation factors,[21,27,30] along with methods to minimize and correct for effects of dielectric sample heating from microwave irradiation on the EPR spectra and other advances in theory.[22] On this basis, our group has developed the long-known Overhauser effect into a quantitative NMR relaxometry tool at 9.8 GHz for the purpose of extracting surface water dynamics,[31–36] corresponding to a frequency for resolving molecular dynamics that is at least an order of magnitude higher than that of conventional ^{1}H NMR relaxometry.[2,28]

The Overhauser effect proceeds only when the frequency of the coupled electron–^{1}H spin transitions is matched by the motion of the nuclear-spin-bearing water. This means that if one uses an external magnetic field of 0.35 T, at which the EPR signal of a nitroxide radical resonates at 9.8 GHz, and the ^{1}H NMR signal is at 14.8 MHz, the molecular motion must match 9.8 GHz ± 14 MHz to induce concurrent electron–^{1}H spin flip-flops of close spins. ODNP at this particular magnetic field is therefore sensitive to correlation times on the order of tens to hundreds of picoseconds.[30,32,34,35]

The translational diffusivity of water molecules near a spin-labeled surface, within a distance of 5–10 Å from the electron spin and encompassing approximately two to four

https://doi.org/10.1557/mrs.2014.254 Published online by Cambridge University Press

water layers, meets these criteria. As long as the water molecules are sufficiently dynamic for their motion to serve as the dominant relaxation mechanism for inducing spin transitions, the diffusive motion of hydration water near a tethered spin probe can be extracted. This analysis requires the application of a dynamic model, with the most commonly used force-free-hard-sphere model best justified for solvent-exposed surfaces, where contributions from bound water populations are minimal or small.[29] As specific solution conditions, such as added cosolvents, buffer molecules, and ions, can affect the local diffusivity of water near spin probes, relative measurements are sometimes necessary to unambiguously report on variations in water diffusion induced by surface properties, as spin probes can perturb the nearby water structure under certain solution conditions.

Thus, the change in local diffusion relative to the translational diffusion of water near a freely dissolved spin probe dissolved in the same bulk water solution, previously termed the diffusion retardation factor, ρ_t, is recorded. Note that all contributions from rapidly diffusing water are isotropically averaged so that ODNP cannot capture anisotropic diffusion properties, for example, parallel versus perpendicular to a surface.[37] Future development of ODNP techniques will permit the exploration of different time scales for correlation times ranging from a few picoseconds to several nanoseconds, when the magnetic field strength is tuned to lower or higher magnetic fields than 0.35 T, which will tune the EPR to frequencies lower or higher than 9.8 GHz.

ODNP has successfully been used to measure surface and local water diffusivities averaged within ~10 Å of electron spin probes near surfaces of globular and membrane proteins, LUVs, nucleic acids, polymers, and solid particles with spatial and temporal selectivity that was otherwise experimentally inaccessible.[21,31–36] **Table I** lists the water diffusion constants measured by ODNP near various hydrophilic surfaces, including negatively charged, positively charged, and neutral polar surfaces, as well as heterogeneous protein surfaces in solution.[35,38] The water diffusivity near hydrophilic surfaces is usually slower than the bulk water diffusivity of 2.4×10^{-9} m^2/s,[19,39] by varying factors, denoted by ρ_t, of up to ~10 (and only in rare cases are the diffusivities comparable, as observed for DNA surfaces).

Table I. Surface water diffusion constants near various hydrophilic surfaces immersed or dissolved in bulk water.[35,38]

Surface Type (polymer, protein, LUV)	Diffusion Constant ($\times 10^{-10}$ m^2/s)	Retardation Factor ρ_t	Surface Characteristics
Poly-vinylimidazole	11.8	2.0	Positive
Poly-aspartic acid	7.8	3.1	Negative
LUV (DOPG/DOPC)	7.0	3.4	Net negative
LUV (DPPC)	6.9	3.5	Zwitterionic
LUV (DOTAP)	9.0	2.7	Positive
Tau(Δ187) protein	9.6	2.5	Net positive
Mfp151 protein	4.0	6	Net positive

Note: DOPC, 1,2-dioleoyl-*sn*-glycero-3-phosphocholine; DOPG, 1,2-dioleoyl-*sn*-glycero-3-[phospho-*rac*-(1-glycerol)]; DOTAP, *N*-(1-(2,3-dioleoyloxy)propyl)-*N*,*N*,*N*-trimethylammonium chloride; DPPC, 1,2-dipalmitoyl-*sn*-glycero-3-phosphatidylcholine; LUV, unilamellar vesicle.

Surface hydration structure and dynamics

The interface between a macromolecular or macroscopic surface in aqueous solution and the surrounding bulk water is broadly termed the hydration layer or the hydration shell of a surface, as long as it forms contiguous bonds with the surrounding water molecules (i.e., is hydrated). Even though hydration layers can consist of the same molecular mixture as the bulk solvent, key properties such as density, directionality, and proportions of weak and strong hydrogen bonds can differ significantly between the bulk solvent and the hydration layer, which can vary from surface to surface as well as from site to site at the nanometer scale.[37,40,41] Charged surfaces, polar surfaces, and surfaces made of hydrogen-bond donors/acceptors mostly constitute hydrophilic surfaces. However, this is not always the case, as illustrated with barely soluble peptides composed of amino acid residues that are considered hydrophilic on average, depending on their primary sequence. Generally, attraction through hydrogen bonds or electrostatic interactions has to be strengthened, not just between water and the hydrophilic surface, but also between water molecules near a surface to achieve an overall strongly hydrophilic surface; we have limited our experimental studies to such surfaces. Water molecules near a hydrophilic surface are observed to have higher densities (<20%)[42–46] and longer diffusion correlation times (>100%)[17,47–51] than bulk water, with the decay length of a hydrophilic surface's hydration shell to bulk solvent dynamics ranging from 0.2 nm to 1.5 nm.[52–54]

In contrast, hydrophobic surface regions or sites can be characterized by stronger water–water than water–surface interactions for water molecules near the surface. Even surfaces or regions conventionally termed hydrophobic, such as surfaces of polystyrene beads or protein regions lined by aromatic residues, do not necessarily repel water; in fact, they often weakly interact with water through van der Waals forces. The potential increase in dangling bonds due to hydrogen-bond breaking near a hydrophobic surface can sometimes encourage the strengthening of other hydrogen bonds and the formation of an "ice-like" hydrogen-bond network surrounding the hydrophobic region, displaying a lower density than bulk water, greater tetrahedral order at lower temperature,[55–59] lower enthalpy and entropy,[60] and/or retarded water dynamics,[61,62] although it can sustain length scales spanning up to,

https://doi.org/10.1557/mrs.2014.254 Published online by Cambridge University Press

in rare cases, 35 nm.[63] However, this ordered water structure will disappear with increasing temperature,[56] as entropic effects come to dominate, and also with the size of the hydrophobic region, as it becomes difficult to form networks of this manner near increasingly large hydrophobic surfaces,[64,65] although even such basic concepts are still debated. We project that disordering and overall weakening of hydrogen bonds will increase the translational diffusion of water near such surfaces.

Note, however, that such measurements of surface water dynamics are experimentally feasible only for hydrophobic regions that are part of an overall hydrated and hydrophilic surface, given experimental constraints of sensitivity and sample preparation. At the same time, any macromolecular surface in solution or practical material surface of interest operating in aqueous environments will be heterogeneous, with nonuniform surface hydrophilicity and hydrophobicity characteristics spanning the whole surface.[11–13] This makes predicting surface hydration water properties highly difficult, as regions displaying faster versus slower water diffusivity might be adjacent to each other, where the local hydration structure is affected not only by the surface but also by the structural arrangement of surrounding water molecules and the synergy between these locally heterogeneous water populations.[66,67]

Surface water diffusion decoupled from bulk water viscosity

To corroborate the unequivocal experimental access to local and surface water distinct from bulk water dynamics by ODNP measurements and explore their dependence on molecular—as opposed to global—effects, the surface water diffusivities, and thus the local water "viscosities," of the hydration layers of LUVs and multilamellar vesicles (MLVs) were probed by ODNP before and after the addition of various viscogens. These are specific molecular additives that enhance the bulk viscosity of the solvent, such as sucrose and glycerol.[25] LUVs and MLVs are self-assemblies of lipid molecules. Whereas an LUV forms a closed membrane of a single bilayer, an MLV forms a stack of bilayers. An LUV serves as a simple model system in solution state that displays a homogeneous hydrophilic surface. The questions investigated were whether the local surface water viscosity, derived from surface water diffusivity, would scale with the bulk water viscosity as systematically altered by the viscogen concentration whose concentration-viscosity relation is known, or whether this surface-to-global-viscosity relationship would depend on the particular viscogen used for changing the bulk viscosity.

In order to enable these studies, nitroxide spin labels were sited off the choline group of 1,2-dioleoyl-*sn*-glycero-3-phosphocholine (DOPC), 1,2-dipalmitoyl-*sn*-glycero-3-phosphatidylcholine (DPPC), or the mixed lipid LUVs so that the solvent volume within 5–10 Å above the phosphate level can be probed by ODNP.[25] Not surprisingly, it was not only found that the local surface viscosity of LUVs was decoupled from the bulk solvent viscosity, but also that the extent of coupling depends dramatically on the surface activity of the viscogens employed, as modulated by the size of the viscogen and the interaction energy between the viscogen and the liposome surface.

Different viscogens, such as Ficoll and sucrose, were chosen to prepare different solutions of the LUV with 10-fold increased solvent viscosity compared to bulk water ($\eta = 10$). The main variance between the viscogens was in physical size and activity coefficients. The local solvent viscosity of the hydration layer at the DPPC head groups of the LUVs was found to increase by, at most, a factor of 2.3, despite a 10-fold increase in bulk viscosity. This decoupling of surface hydration water from bulk water held true in the cases of both Ficoll and sucrose, with sucrose imposing a larger influence. The interaction between the particular viscogen and the bulk-water-exposed LUV liposome surface, not the bulk water viscosity, was confirmed to play a critical role in tuning the surface water viscosity, a concept that was experimentally confirmed for the first time with ODNP-based measurements of surface water diffusivity.[34]

What about nanometer-scale confinements that are intuitively thought to be a key modulator of the effective water diffusivity? By performing the same measurements on MLV systems, where the interstitial solvent region spanning 1–1.5 nm can be investigated by liposome-surface-attached spin probes, physical confinement at the nanometer scale alone it was seen that did not significantly influence the intrinsic, short-time-limit surface hydration water diffusivity. In the competition between nanoscale confinements, the chemical properties of the surface, and the physical crowding of the bulk solution, the hydration water dynamics at LUV surfaces and MLV interfaces were found to be primarily determined by the surface properties.[25]

Modulated surface water diffusion and activation energy

The activation energy for water diffusion contains information on the local hydration structure[35] and can be derived near hydrophilic surfaces or in bulk water by examining the temperature dependence of the diffusion coefficient. The Arrhenius plot of ODNP-measured bulk water diffusion as a function of temperature was shown to reproduce the bulk water diffusion activation energy of 19 kJ/mol, although reporting a significantly higher diffusion activation energy for water within the hydration shell of hydrophilic LUV surfaces (27 kJ/mol for DPPC and 31 kJ/mol for DOTAP LUV surfaces, where DOTAP is *N*-(1-(2,3-dioleoyloxy)propyl)-*N*,*N*,*N*-trimethylammonium chloride).[19] Together with the measurement of a retarded surface water diffusion coefficient, this verifies that the water molecules near hydrophilic LUV surfaces experience greater adhesive and cohesive interactions than those in bulk water.

Assuming similar hydration structures and environments, such as a known reference in the same hydration shell, the change in water diffusion activation energy can also be extracted from the local water diffusion constant determined by ODNP, without the need to record the temperature dependence explicitly.[33]

https://doi.org/10.1557/mrs.2014.254 Published online by Cambridge University Press

Figure 1 presents the changes in the local water diffusion activation energy, derived in this manner for the hydration shell of 1-palmitoyl-2-oleoyl-*sn*-glycero-3-phosphocholine (POPC) LUVs upon addition to bulk water of specific ions at relatively dilute (100 mM) concentrations. Interestingly, the surface water diffusion activation energy of this hydration shell changed as ions were added to the pure water dissolving the LUVs, with the extent and direction of change varying with the type of ion following a specific order, the Hofmeister series.[68,69] The Hofmeister series is the order of various ions, ranked by the ion's ability to change the co-solute macromolecular interaction. That diffusion activation energies of water, thought to reflect surface hydrophilicity, could track with the Hofmeister series is novel yet plausible, considering that Hofmeister ions are known to induce changes in hydrated polymer surfaces[70] that ultimately modulate the polymer–polymer versus polymer–water interaction balance, leading to the dissolution versus aggregation of a broad range of polymers and proteins.

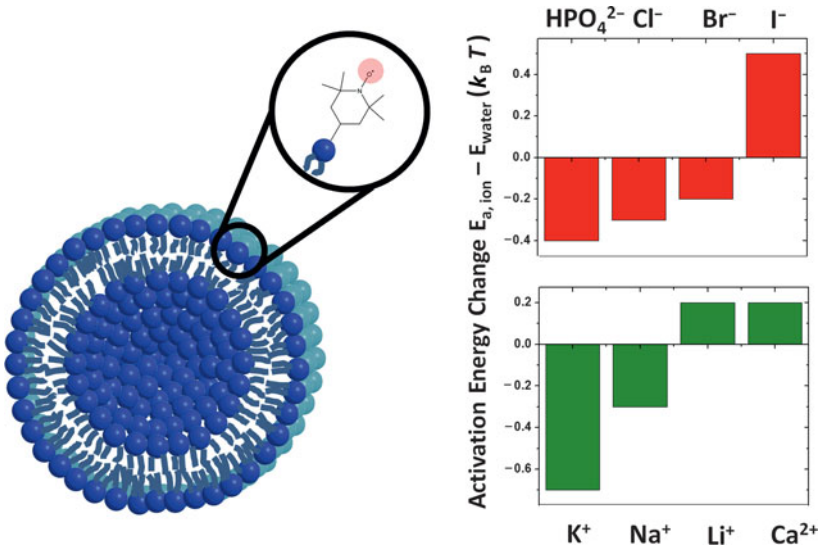


Figure 1. Changes in the diffusion activation energy of water at the hydration layer of 1-palmitoyl-2-oleoyl-*sn*-glycero-3-phosphocholine (POPC) unilamellar vesicles (LUVs). The water diffusion activation energy at the POPC surface without added electrolyte was set to 0 k_BT. Reproduced with permission from Reference 33. © 2014 American Chemical Society.

Heterogeneous protein surface water diffusion landscape

The benefit of ODNP as a local water dynamics probe can be further illustrated by the site-specific probing of a heterogeneous protein surface, such as that of the globular apomyoglobin protein, an external α-helical loop of proteorhodopsin,[36,71] and α-synuclein embedded at the membrane interface (**Figure 2**).[23] Proteorhodopsin and α-synuclein are membrane embedded or associating proteins that function in lipid membrane environments. Depending on where the spin label was located, ODNP probed dramatically diverse local water diffusion constants, denoted in terms of a retardation factor, ρ_t, from the bulk water diffusion constant of 2.4×10^{-9} m^2/s,[19,39] ranging from 3 to 10 in the case of lipid-embedded α-synuclein. The smaller the retardation factor, the faster the local water diffusion.

Here, we need to differentiate two distinct scenarios for the origin of diverse retardation factors for surface water diffusion: (1) different solvent accessibility that alters the distance of closest approach between water and the spin probe and (2) spatially varying surface hydrophilicity giving rise to different hydration structures. For the α-helical portion of α-synuclein, it is known explicitly, from power-saturation EPR measurements in the

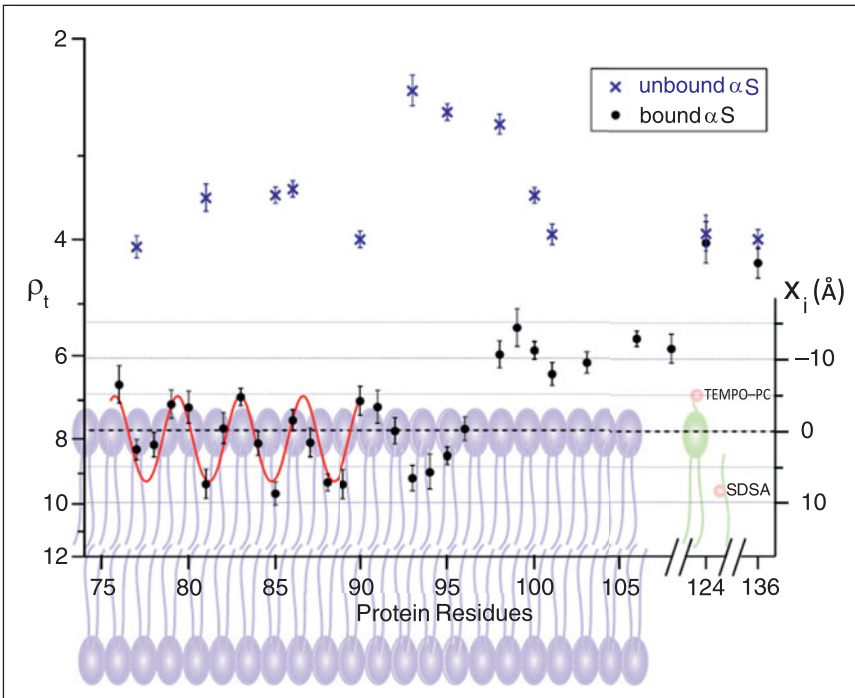


Figure 2. Retardation factor (ρ_t) at various residues of membrane-bound and free α-synuclein (αS) as measured by Overhauser dynamic nuclear polarization (ODNP). The distance (x_i) of nitroxide spin probes relative to the phosphate group of 1-palmitoyl-2-oleoyl-*sn*-glycero-3-phosphocholine/1-palmitoyl-2-oleoyl-*sn*-glycero-3-phosphoserine bilayers is presented together with ρ_t. The lipid spin probes used for ODNP are shown to the right, with the nitroxide radicals represented as red balls. Reproduced with permission from Reference 31. © National Academy of Sciences. Note: SDSA, structure-dependent sequence alignment; TEMPO-PC, 1,2-dipalmitoyl-*sn*-glycero-3-phospho(TEMPO) choline.

https://doi.org/10.1557/mrs.2014.254 Published online by Cambridge University Press

literature,[72] that the water accessibility periodically varies concurrently with the ODNP-derived ρ_t factor.[73,74] However, it is also known explicitly that amino acid residues 97–136 of α-synuclein are bulk-water-exposed, while still presenting significant variability for ρ_t values between 4 and 6. In this case, it is due to different hydration structure, as modulated by the proximity and property of the adjacent surface, here the LUV. The ability to resolve heterogeneities of surface water structure and dynamics of protein surfaces will contribute to unraveling the hotly debated question of the functional role of surface water properties in possibly (passively or actively) mediating protein interaction and catalysis.[75–78]

Role of surface water hydrophilicity in material function

Heterogeneities of surface hydration dynamics properties are also present on material surfaces and are thought to play an important role in their function, although not as delicately tuned and perfectly choreographed as on structured protein surfaces. Membrane materials that are designed to pump ions or water across their channels require structural and chemical heterogeneities to ensure mechanical stability and high percolation, as well as optimal hydration and transport at the same time. Taking a Nafion fuel cell membrane as an example, sulfonic acid groups are needed to hydrate the channels, but they are also known to play a key role in mediating rapid proton transfer, while water needs to be efficiently drained in the direction opposite to proton transport.[16] This suggests that very hydrophilic surfaces might exert too strong an attractive force on surface water, hindering separation from the membrane surface, whereas insufficiently hydrophilic surfaces will not swell optimally to generate the needed water channels. The existence of a uniform hydrophilic surface that can play both roles is unlikely. Rather, chemical heterogeneities, such as provided by the sulfonic acid groups and fluorinated Teflon polymer surfaces, can work in concert to impart such complex functionality to membrane materials. This consideration is generally valid for other functional materials operating in water that need to balance adsorption and reaction against transport and dynamics, such as separation and reaction columns, water-based heterogeneous catalysis, and other membrane materials.

Experimental access to locally varying surface hydrophilicity by site-specific ODNP measurements can also become important for evaluating the effect of surface micropatterning.[79–82] On highly heterogeneous surfaces, local properties can differ at the nanometer scale[83–85] and present junction zones.[86] For many materials, the measurement of the average surface water properties might not be sufficient to explain even macroscopic properties of a heterogeneous surface,[87,88] with a delicate balance needed between surface–water attraction and repulsion to achieve overall optimal ion and water transport in fuel cell membranes serving as an illustrative example. Generally, whenever the correlation and collective behavior of the surface[89] and the resulting correlation with hydration structure[85,86] are important, the local hydration structure can change the effective surface hydrophilicity.[66,67]

Here, the ODNP-derived local water diffusivity offers the opportunity to experimentally measure local hydrophilicity near different surfaces and can help reveal how (sub-) nanometer-scale variances in chemical properties, topology, and surface composition can alter the effective local surface properties; such effects cannot be easily predicted from average surface chemistry. Consider a globular protein whose surface topology and composition are "perfectly" known: Even something as seemingly basic as its net hydrophilicity, as manifested in protein solubility, cannot be easily predicted, let alone subtle features such as the protein binding interface or active site. We conclude that the ODNP methodology will offer valuable empirical insight into what determines the surface hydrophilicity of a host of materials and biological surfaces in solution and their potential functional roles, as well as critical experimental data for computational studies to fill the gap to address the ultimate question of what the molecular "alphabet and language" is for determining and tuning the surface water hydration dynamics landscape of materials and biological systems.

Acknowledgments

This research was supported by the 2011 NIH Directors New Innovator Award and the Packard Fellowship awarded to S.H. The authors made use of the Materials Research Laboratory Central Facilities, supported by the National Science Foundation through an MRSEC under Grant DMR 1121053. John Franck is acknowledged for developing the ODNP hardware and software platform that enabled the studies.

References

1. B. Bagchi, *Chem. Rev.* **105**, 3197 (2005).
2. J. Qvist, E. Persson, C. Mattea, B. Halle, *Faraday Discuss.* **141**, 131 (2009).
3. A. Dey, F.E. Jenney Jr., M.W.W. Adams, E. Babini, Y. Takahashi, K. Fukuyama, K.O. Hodgson, B. Hedman, E.I. Solomon, *Science* **318**, 1464 (2007).
4. I. Brovchenko, A. Oleinikova, *ChemPhysChem* **9**, 2695 (2008).
5. A. Fernández, H.A. Scheraga, *Proc. Natl. Acad. Sci. U.S.A.* **100**, 113 (2003).
6. M. Heyden, D.J. Tobias, *Phys. Rev. Lett.* **111**, 218101 (2013).
7. D. Russo, J. Teixeira, L. Kneller, J.R.D. Copley, J. Ollivier, S. Perticaroli, E. Pellegrini, M.A. Gonzalez, *J. Am. Chem. Soc.* **133**, 4882 (2011).
8. Y. Yuan, T.R. Lee, in *Surface Science Techniques*, G. Bracco, B. Holst, Eds., Springer Series in Surface Sciences (Springer, Berlin, 2013), vol. 51, pp. 3–34.
9. B.S. Marques, N.V. Nucci, A.J. Wand, *Biophys. J.* **104**, 180A (2013).
10. N.V. Nucci, M.S. Pometun, A.J. Wand, *Nat. Struct. Mol. Biol.* **18**, 245 (2011).
11. J. DeFelipe, *Cereb. Cortex* **3**, 273 (1993).
12. R.A. Vijayendran, D.E. Leckband, *Anal. Chem.* **73**, 471 (2001).
13. R.D. Johnson, F.H. Arnold, *Biochim. Biophys. Acta* **1247**, 293 (1995).
14. E.W. Knapp, I. Muegge, *J. Phys. Chem.* **97**, 11339 (1993).
15. P. Huetz, V. Ball, J.-C. Voegel, P. Schaaf, *Langmuir* **11**, 3145 (1995).
16. K.A. Mauritz, R.B. Moore, *Chem. Rev.* **104**, 4535 (2004).
17. D. Zhong, S.K. Pal, A.H. Zewail, *Chem. Phys. Lett.* **503**, 1 (2011).
18. R. Helmy, A.Y. Fadeev, *Abstr. Pap. Am. Chem. Soc.* **229**, U708 (2005).
19. J.H. Wang, C.V. Robinson, I.S. Edelman, *J. Am. Chem. Soc.* **75**, 466 (1953).
20. B.D. Armstrong, S. Han, *J. Chem. Phys.* **127**, 104508 (2007).
21. B.D. Armstrong, J. Choi, C. Lopez, D.A. Wesener, W. Hubbell, S. Cavagnero, S. Han, *J. Am. Chem. Soc.* **133**, 5987 (2011).
22. J.M. Franck, A. Pavlova, J.A. Scott, S. Han, *Prog. Nucl. Magn. Reson. Spectrosc.* **74**, 33 (2013).
23. A.W. Overhauser, *Phys. Rev.* **92**, 411 (1953).
24. A. Abragam, *Principles of Nuclear Magnetism* (Oxford University Press, Oxford, UK, 1961).
25. I. Solomon, *Phys. Rev.* **99**, 559 (1955).
26. K.H. Hausser, D. Stehlik, *Adv. Magn. Reson.* **127**, 79 (1968).

https://doi.org/10.1557/mrs.2014.254 Published online by Cambridge University Press

27. M.-T. Turke, I. Tkach, M. Reese, P. Hofer, M. Bennati, *Phys. Chem. Chem. Phys.* **12**, 5893 (2010).
28. M.W. Hodges, D.S. Cafiso, C.F. Polnaszek, C.C. Lester, R.G. Bryant, *Biophys. J.* **73**, 2575 (1997).
29. J.H. Freed, *J. Chem. Phys.* **68**, 4034 (1978).
30. R.D. Bates Jr., W.S. Drozdoski, *J. Chem. Phys.* **67**, 4038 (1977).
31. C.-Y. Cheng, J. Varkey, M.R. Ambroso, R. Langen, S. Han, *Proc. Natl. Acad. Sci. U.S.A.* **110**, 16838 (2013).
32. C.-Y. Cheng, S. Han, *Annu. Rev. Phys. Chem.* **64**, 507 (2013).
33. J. Song, J. Franck, P. Pincus, M.W. Kim, S. Han, *J. Am. Chem. Soc.* **136**, 2642 (2014).
34. J.M. Franck, J.A. Scott, S. Han, *J. Am. Chem. Soc.* **135**, 4175 (2013).
35. R. Kausik, S. Han, *J. Am. Chem. Soc.* **131**, 18254 (2009).
36. S. Hussain, J.M. Franck, S. Han, *Angew. Chem. Int. Ed.* **52**, 1953 (2013).
37. S.H. Lee, P.J. Rossky, *J. Chem. Phys.* **100**, 3334 (1994).
38. J.H. Ortony, C.-Y. Cheng, J.M. Franck, R. Kausik, A. Pavlova, J. Hunt, S. Han, *New J. Phys.* **13**, 015006 (2011).
39. C.A. Wraight, *Biochim. Biophys. Acta* **1757**, 886 (2006).
40. A.P. Dabkowska, F. Foglia, M.J. Lawrence, C.D. Lorenz, S.E. McLain, *J. Chem. Phys.* **135**, 225105 (2011).
41. J. Wang, A.G. Kalinichev, R.J. Kirkpatrick, *J. Phys. Chem. C* **113**, 11077 (2009).
42. D.I. Svergun, S. Richard, M.H.J. Koch, Z. Sayers, S. Kuprin, G. Zaccai, *Proc. Natl. Acad. Sci. U.S.A.* **95**, 2267 (1998).
43. F. Merzel, J.C. Smith, *Proc. Natl. Acad. Sci. U.S.A.* **99**, 5378 (2002).
44. J.C. Smith, F. Merzel, C.S. Verma, S. Fischer, *J. Mol. Liq.* **101**, 27 (2002).
45. M. Levitt, R. Sharon, *Proc. Natl. Acad. Sci. U.S.A.* **85**, 7557 (1988).
46. S. Chakraborty, S.K. Sinha, S. Bandyopadhyay, *J. Phys. Chem. B* **111**, 13626 (2007).
47. H. Xu, B.J. Berne, *J. Phys. Chem. B* **105**, 11929 (2001).
48. M. Marchi, F. Sterpone, M. Ceccarelli, *J. Am. Chem. Soc.* **124**, 6787 (2002).
49. T. Yokomizo, S. Yagihara, J. Higo, *Chem. Phys. Lett.* **374**, 453 (2003).
50. V.A. Makarov, B.K. Andrews, P.E. Smith, B.M. Pettitt, *Biophys. J.* **79**, 2966 (2000).
51. V. Makarov, B.M. Pettitt, *Acc. Chem. Res.* **35**, 376 (2002).
52. B.J. Smith, A. Rawal, G.P. Funkhouser, L.R. Roberts, V. Gupta, J.N. Israelachvili, B.F. Chmelk, *Proc. Natl. Acad. Sci. U.S.A.* **108**, 8949 (2011).
53. E. Schneck, B. Deme, C. Gege, M. Tanaka, *Biophys. J.* **100**, 2151 (2011).
54. J.N. Israelachvili, *Intermolecular and Surface Forces*, 2nd ed. (Academic Press, San Diego, CA, 1991).
55. H.J. Bakker, *Nature* **491**, 533 (2012).
56. J.G. Davis, K.P. Gierszal, P. Wang, D. Ben-Amotz, *Nature* **491**, 582 (2012).
57. K.R. Wilson, R.D. Schaller, D.T. Co, R.J. Saykally, B.S. Rude, T. Catalano, J.D. Bozek, *J. Chem. Phys.* **117**, 7738 (2002).
58. R. Steitz, T. Gutberlet, T. Hauss, B. Klosgen, R. Krastev, S. Schemmel, A.C. Simonsen, G.H. Findenegg, *Langmuir* **19**, 2409 (2003).
59. T.R. Jensen, M.Ø. Jensen, N. Reitzel, K. Balashev, G.H. Peters, K. Kjaer, T. Bjørnholm, *Phys. Rev. Lett.* **90**, 086101 (2003).
60. T.V. Chalikian, *J. Phys. Chem. B* **105**, 12566 (2001).
61. J.T. Titantah, M. Karttunen, *J. Am. Chem. Soc.* **134**, 9362 (2012).
62. Y.L.A. Rezus, H.J. Bakker, *Phys. Rev. Lett.* **99**, 148301 (2007).
63. Y.I. Tarasevich, *Colloid J.* **73**, 257 (2011).
64. D. Chandler, *Nature* **437**, 640 (2005).
65. A.J. Patel, J.N. Sarkaria, S.H. Kaufmann, *Proc. Natl. Acad. Sci. U.S.A.* **108**, 17678 (2011).
66. N. Giovambattista, P.G. Debenedetti, P.J. Rossky, *J. Phys. Chem. C* **111**, 1323 (2007).
67. N. Giovambattista, P.G. Debenedetti, P.J. Rossky, *Proc. Natl. Acad. Sci. U.S.A.* **106**, 15181 (2009).
68. F. Hofmeister, *Arch. Exp. Pathol. Pharmakol.* **24**, 247 (1888).
69. W. Kunz, *Specific Ion Effects* (World Scientific, Singapore, 2010).
70. Y. Zhang, S. Furyk, D.E. Bergbreiter, P.S. Cremer, *J. Am. Chem. Soc.* **127**, 14505 (2005).
71. K.M. Stone, J. Voska, M. Kinnebrew, A. Pavlova, M.J.N. Junk, S. Han, *Biophys. J.* **104**, 472 (2013).
72. C.C. Jao, A. Der-Sarkissian, J. Chen, R. Langen, *Proc. Natl. Acad. Sci. U.S.A.* **101**, 8331 (2004).
73. C. Altenbach, D.A. Greenhalgh, H.G. Khorana, W.L. Hubbell, *Proc. Natl. Acad. Sci. U.S.A.* **91**, 1667 (1994).
74. C.C. Jao, B.G. Hegde, J. Chen, I.S. Haworth, R. Langen, *Proc. Natl. Acad. Sci. U.S.A.* **105**, 19666 (2008).
75. P. Ball, *Chem. Rev.* **108**, 74 (2008).
76. M. Chaplin, *Nat. Rev. Mol. Cell Biol.* **7**, 861 (2006).
77. P.W. Fenimore, H. Frauenfelder, B.H. McMahon, F.G. Parak, *Proc. Natl. Acad. Sci. U.S.A.* **99**, 16047 (2002).
78. Y. Levy, J.N. Onuchic, *Annu. Rev. Biophys. Biomol. Struct.* **35**, 389 (2006).
79. J.K. Cox, A. Eisenberg, R.B. Lennox, *Curr. Opin. Colloid Interface Sci.* **4**, 52 (1999).
80. K. Lee, F. Pan, G.T. Carroll, N.J. Turro, J.T. Koberstein, *Langmuir* **20**, 1812 (2004).
81. M.P. Stoykovich, M. Muller, S.O. Kim, H.H. Solak, E.W. Edwards, J.J. de Pablo, P.F. Nealey, *Science* **308**, 1442 (2005).
82. Y. Okabea, S. Kurihara, T. Yajima, Y. Seki, I. Nakamura, I. Takano, *Surf. Coat. Technol.* **196**, 303 (2005).
83. K.A. Dill, *Biochemistry* **29**, 7133 (1990).
84. H. Gau, S. Herminghaus, P. Lenz, R. Lipowsky, *Science* **283**, 46 (1999).
85. P.L. Privalov, G.I. Makhatadze, *J. Mol. Biol.* **232**, 660 (1993).
86. C.-Y. Ruan, V.A. Lobastov, F. Vigliotti, S. Chen, A.H. Zewail, *Science* **304**, 80 (2004).
87. J. Bico, C. Marzolin, D. Quere, *Europhys. Lett.* **47**, 220 (1999).
88. T. Sun, G. Wang, H. Liu, L. Feng, L. Jiang, D. Zhu, *J. Am. Chem. Soc.* **125**, 14996 (2003).
89. L. Lu, M.L. Berkowitz, *J. Chem. Phys.* **124**, 101101 (2006). □



https://doi.org/10.1557/mrs.2014.254 Published online by Cambridge University Press